Title

Exposure Assessment For Air-To-Skin Uptake of Semivolatile Organic Compounds (SVOCs) Indoors

Journal

Environmental Science and Technology, 53(3)

ISSN

0013-936X

Authors

Garrido, Javier A
Parthasarathy, Srinandini
Moschet, Christoph
et al.

Publication Date

2019-02-05

DOI

10.1021/acs.est.8b05123

Peer reviewed

HHS Public Access

Author manuscript

Environ Sci Technol. Author manuscript; available in PMC 2020 February 23.

Published in final edited form as:

Environ Sci Technol. 2019 February 05; 53(3): 1608–1616. doi:10.1021/acs.est.8b05123.

Exposure Assessment For Air-To-Skin Uptake of Semivolatile Organic Compounds (SVOCs) Indoors

Javier A. Garrido[a], **Srinandini Parthasarathy**[b], **Christoph Moschet**[c,⊥], **Thomas M. Young**[c], **Thomas E. McKone**[b,d], **Deborah H. Bennett**[e]

[a]Forensic Science Graduate Program, University of California, Davis, California, USA

[b]Department of Environmental Health Sciences, School of Public Health, University of California, Berkeley, California, USA

[c]Department of Civil and Environmental Engineering, University of California, Davis, California, USA

[d]Energy Analysis and Environmental Impacts Division, Lawrence Berkeley National Laboratory, Berkeley, California, USA

[e]Department of Public Health Sciences, University of California, Davis, California, USA

Abstract

Semi-volatile organic compounds (SVOCs) are ubiquitous in the indoor environment and a priority for exposure assessment because of the environmental health concerns that they pose. Direct air-to-skin dermal uptake has been shown to be comparable to the inhalation intake for compounds with certain chemical properties. In this study, we aim to further understand the transport of these types of chemicals through the skin, specifically through the stratum corneum (SC). Our assessment is based on collecting three sequential forehead skin wipes, each hypothesised to remove pollutants from successively deeper skin layers, and using these wipe analyses to determine the skin concentration profiles. The removal of SVOCs with repeated wipes reveals the concentration profiles with depth and provides a way to characterize penetration efficiency and potential transfer to blood circulation. We used a diffusion model applied to surface skin to simulate concentration profiles of SVOCs and compared them with the measured values. We found that two phthalates, dimethyl and diethyl phthalates, penetrate deeper into skin with similar exposure compared to other phthalates and targeted SVOCs--an observation supported by the model results as well. We also report the presence of statistically significant declining patterns with skin depth for most SVOCs, indicating that their diffusion through the SC is relevant and eventually can reach the blood vessels in the vascularized dermis. Finally, using a non-target approach, we identified skin oxidation products, linked to respiratory irritation symptoms, formed from the reaction between ozone and squalene.

Graphical Abstract

Contact: dhbennett@ucdavis.edu.

⊥present address: Interkantonales Labor, Schaffhausen, Mühlentalstrasse 188, CH-8200 Schaffhausen, Switzerland.

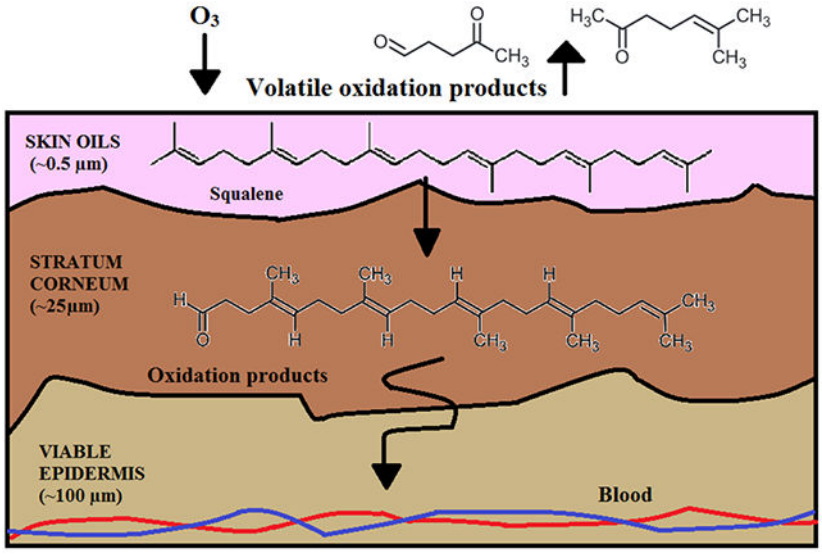

INTRODUCTION

Semi-volatile organic compounds (SVOCs) are ubiquitous in the indoor environment [1] with building materials, such as flooring, walls and upholstery, furniture, electronics, consumer and personal care products acting as sources. As a result of their chemical properties and low vapor pressures, once released from sources, SVOCs partition into indoor surfaces and dust, raising concerns about human exposure through dermal uptake and non-dietary ingestion. This is particularly important for children, due to their frequent contact with surfaces and hand-to-mouth activities. Previous toxicological and epidemiological studies [2-6] have documented adverse health effects associated with childhood exposure to SVOCs. In addition to surface contact-driven uptake [7], there is growing concern regarding direct dermal uptake from air [8], as the dermal pathway has been less studied and may contribute more to cumulative indoor intake than previously thought. When exposure occurs through the dermal route, the chemical is directly passed into the bloodstream, with minimal metabolism in the skin layers [9] , reaching target organs and shunting the intestinal absorption or airway passages.

Dermal exposure to indoor chemicals can occur either by direct contact with a surface or by direct transdermal uptake from air [8, 10, 11]. This latter process occurs similarly to the process of partitioning between air and organic matter on indoor surfaces [8]. After partitioning directly from air into the skin, SVOCs can permeate through the skin, and depending on their chemical properties, go deep enough to pass into the bloodstream. This process has been documented with transdermal delivery of pharmaceuticals, which, because of their similar chemical properties, can be classified as SVOCs [12].

There is a long-established record of research on the importance of the air-to-skin transfer pathway for volatile organic compounds (VOCs), with some studies demonstrating that uptake through this route provides a significant proportion of the total intake of these compounds, especially industrial solvents [13, 14], such as phenol, nitrobenzene and gas

phase glycol ethers [15-19].. More recently, other studies have shown significant dermal uptake of benzophenone-3 (BP-3) and nicotine from clothing that has reached equilibrium with nearby air , as shown with measurements in biofluids. For nicotine, the dermal uptake can be greater than inhalation rates [20].

Recently, models that capture air-to-skin uptake of SVOCs have clearly demonstrated their potential to partition into skin similarly to VOCs [1]. Theoretical estimates indicate that, for SVOCs with high octanol-air partition coefficients (K_{oa}), the chemical mass in 10 to 20 m^3 of indoor air can be removed by skin per hour, significantly higher than the typical inhalation intake of 1 m^3/h. These models have been confirmed with experiments quantifying the direct dermal uptake of airborne SVOCs [11, 21]. Weschler et al. 2015 [11], used a chamber to provide controlled exposures to people with bare arms and legs to different phthalates and then measured biomarkers in urine and blood and found that the dermal uptake route was comparable to the inhalation route. The role of clothing has also been studied [20, 22, 23] with the conclusion that clothing can be protective if it is cleaned and not previously exposed to the chemical; however the effect is contingent on the type of chemical (for nicotine it was different than for phthalates) and whether the model considered skin surface lipids (SSL) or not.

More recently, improved models for dermal uptake from air include a boundary resistance layer through air [24], providing a “transient” mass-transfer approach that enables estimation of dermal exposures under dynamic conditions [1, 8, 11, 21, 25]. These models have been partially validated [24, 26, 27] using data from studies where individuals had skin exposed to gas-phase compounds and absorbed dose was calculated by measuring levels in biofluids. There is ample evidence documenting the importance of the air to skin transfer of chemicals, but more insight is needed to accurately describe the diffusion of compounds through the skin once they have partitioned onto the surface.

Another recently-studied phenomenon is the impact of occupants on indoor chemistry [28] . It has been reported that skin lipids react with indoor ozone to form oxidation by-products [29, 30] that can alter the indoor chemistry. These substances can affect the oxidative capacity of indoor air, since the by-products react with different radicals and oxidants present (such as hydroxyl radicals), reducing their concentrations [28]. . As a result of these skin-lipid reactions, indoor ozone concentrations decrease, which can in turn impact the composition and concentration of secondary organic aerosols (SOA) [31], an important fraction of particulate matter indoors. Furthermore, the more volatile oxidation by-products, such as 4-oxo pentanal, can concentrate in the air and act as respiratory irritants [32]. Other low-volatility products can accumulate in skin oils and act as skin irritants, with the potential of being absorbed into the bloodstream [33].. By recognizing the reaction between squalene and ozone, we found that the identification of the oxidation products and the analysis of their concentration gradient as revealed by consecutive skin wipe from our experiments offers an additional opportunity to study this emerging issue of indoor chemistry.

In this study, we use multiple consecutive forehead wipes to further study and better understand transport of SVOCs through the SC and the potential for their absorption into the bloodstream. We used a diffusion model [1] to describe the transport of selected SVOCs

through the SC, the layer that offers the highest resistance to diffusion and transport through the skin. We then compare empirical data collected from individuals to the model predictions and estimate the depth of sampling associated with each wipe using the distribution of squalene concentrations measured in the participants. Lastly, we used a non-target approach to determine the presence of squalene oxidation products in the wipes to explore this new area of indoor air chemistry to determine if these compounds penetrate into the skin. To the best of our knowledge, this is the first study that utilizes quantitative information from multiple skin wipes to explore the fate of SVOCs in skin

METHODS

In the paragraphs below, we present our methods for the field collection measurements, dermal model development and evaluation, and methods for identification of ozone reaction products.

Study design

We recruited 13 subjects for our wipe sampling study. The subjects were all adults 18 years of age or older from Northern California. The group included 7 men and 6 women and represented a convenience sample. The same individual collected all samples following a standardized protocol to reduce experimental variability. The study was conducted under the University of California, Davis Institutional Review Board review and approval.

Sample collection and analysis

To study the passive transfer of chemicals to skin from air, we collected sequential skin wipe samples from the forehead, one after another with no time interval in between. The forehead is an area thought to have primarily passive exposure, although hand-to-head contact is a possible route influencing the forehead levels. We refer to the first wipe collected as FH-1, with subsequent wipes being designated as FH-2 and FH-3. Multiple consecutive wipes were taken in a similar manner as part of the QA/QC procedure in a prior study [34]. Each wipe sample was collected using a clean gauze pad, previously soaked in isopropanol, with the samples immediately stored in a cooler for transportation after collection We also collected one hand wipe from the palm and area between fingers per subject, wiping the surface once (HW), in order to provide an estimate of contact-driven transfer of the subject chemicals to skin. Based on a distribution of average forehead sizes, we estimated that the area across which we sampled each participant's forehead was 15 cm^2 [35].

Before use gauze pads (MG Chemicals, Surrey, BC, Canada) were Soxhlet extracted in hexane:acetone (1:1 v/v) for 24 h in batches of 50 wipes. After sample collection, a mixture of different isotope-labelled internal standards was added, the wipes were extracted using a 5 mL, 3:1 mixture of hexane and acetone, and sonicated [36]. After transferring the supernatant, wipes were extracted again by adding 5 mL of acetone and sonicating. The resulting extracts were combined, the sample was evaporated to a final volume of 1 mL, filtered, and split into two fractions, one for the GC-MS analysis, the other for the LC-MS analysis.

We analyzed the GC-MS fraction on a 7200B GC-Q/TOF (quadrupole time-of-flight, high-resolution mass spectrometer, Agilent Technologies Inc.) using a standard column in 80 min chromatographic runs [36]. With this analysis, we quantified 17 targeted SVOCs (Table 1).

For the LC-MS analysis, we solvent transferred the samples to a methanol:water solution (1:1 v/v). We analyzed the LC-MS fraction on a 6530 LC-Q/TOF (Agilent Technologies Inc.) high-resolution mass spectrometer using a reversed phase column in a 24 min chromatographic run and electrospray ionization in positive and negative ionization modes [36].

We also used the data obtained from both the LC and GC in a non-target screen for potential oxidation products [29, 30]. We screened the samples extracted from the wipes for primary oxidation products linked to ozone reaction as listed in Wisthaler and Weschler [29]. In addition, we performed a non-target analysis by suspect/exact masses screening [37] to identify other potential, commonly detected products.

With the acquired high resolution GC-Q/TOF data, we performed non-target screening using the software Unknowns Analysis (B.08 Agilent Technologies). In this approach, we compared non-target peaks detected by spectral deconvolution to the NIST 14 mass spectral library [36, 38].

We performed a suspect screening with the acquired high resolution LC-Q/TOF data. This procedure automatically searched the exact masses and isotopic patterns of seven oxidation products of squalene [29] by the software Masshunter Qual (B.08 Agilent Technologies). For the compounds with a molecular formula match, we reanalyzed the samples in a tandem MS/MS mode in order to form fragments of the molecule and to obtain a specific spectrum. Because authentic standards and library spectra were not available for these compounds, we compared the obtained fragments with predicted fragments from in-silico computer programs (Agilent Molecular Structure Correlator).

Estimation of the depth of each skin wipe and depth patterns of the chemicals

The depth of sampling of each wipe is needed to evaluate the permeation profile of chemicals through the skin. To deduce the depth from which a chemical is removed from the skin by wiping, we compared measured squalene mass recovered in successive wipes to concentrations reported in the literature and then used squalene as a removal marker for the wipes to determine equivalent depth. Typical skin lipid concentrations range from 90 to 120 $\mu g/cm^2$ [39, 40], with higher lipid concentrations in the forehead, 150–300 $\mu g/cm^2$, due to the high density of epidermal glands on the forehead [41]. Based on estimates from Greene et al. [41], squalene can, on average, comprise about 12.3% of the total by mass of skin surface lipids, ranging from 12 to 14%.

We calculated the geometric mean and standard deviation of the depth from which chemical was removed with each skin wipe across individuals, assuming a uniform concentration of squalene (12.3% of a total of 300 $\mu g/cm^2$ of skin lipids in the upper layer of the SC from which squalene is extracted), a lipid density of 1 g/cm^3 [42], a constant area sampled with each wipe (15 cm^2), and the squalene levels in each wipe for each subject. The mean

squalene levels in our population were in good agreement with the 300 μg/cm^2 value. Although squalene concentrations are expected to decrease somewhat with depth of skin, we assumed a constant concentration over the relatively shallow skin depths sampled here, as well as between individuals, to facilitate calculations.

After we estimated the depth of sampling for each wipe, we studied the concentration patterns for each chemical with depth by calculating correlation coefficients between concentrations and estimated sampling depth, ρ, across all subjects, and estimated their significance with a Fisher transformation. We also normalized the FH-2 and FH-3 sample concentrations to the FH-1 sample concentrations. These two methods allow us to explore chemical penetration through the skin.

Model of transport of chemicals in the stratum corneum (SC).

There are two transport processes for a chemical to reach the bloodstream: first, partitioning from air to skin, and second, transport across the SC to the viable epidermis to reach blood vessels.

To derive further insight from the experimental work, we used the model developed by Weschler and Nazaroff [1, 10] (see SI for more details) to estimate the time required for compounds to move from air to skin followed by the transport of chemical substances through the skin based on Fickian diffusion within the SC, specifically evaluating phthalates.

In this approach, we first calculate the equilibrium concentration ratio between the top 1 μm of skin lipids and air, which is derived from the octanol-air partitioning coefficient with the modifications proposed by Weschler and Nazaroff [1, 10]. From a mathematical standpoint, assuming an outer layer that must first come to equilibrium is similar to assuming a skin surface layer (SSL). We also calculated the time to equilibrium for the chemicals to partition from air to surface skin lipids, τ. Calculating first the time for a thin top layer of skin to reach equilibrium with the air, and then separately modeling transport through the skin is a similar concept as the existence of a thin skin surface lipid layer as proposed by Morrison et al.[27].

We next modeled the movement of chemical into skin using a dynamic mass-transfer model [1, 10] that produces a concentration-depth profile within the SC. The SC offers the greatest resistance to movement of chemical through skin as compared to other skin layers. Because there is a lack of direct measurements of skin diffusion coefficients (D_{sc}) available for compounds with log K_{ow} values in the range of most SVOCs, we use permeability coefficient estimation equations from the U.S. EPA dermal exposure guidelines [35]. These equations use K_{ow} and molecular weight values [43, 44] to obtain estimated diffusion coefficients (Table 3).

To compare the relative diffusion through skin to measured results, we calculate the concentrations in the SC after 24 hours of exposure, and we take values at the experimental depth of each wipe. Then we normalize those concentrations to that of the skin surface and compare them to the measured values.

Consistency of compounds between various wipes.

We used Spearman rank correlation coefficients for the hand wipes (HW) and FH-1 to assess the consistency of the chemicals present in these wipes. Also, we developed correlation matrices between the chemicals found in the forehead wipes and the hand wipes to investigate possible common sources and behaviors. The matrices and results can be found in the SI.

RESULTS AND DISCUSSION

Stratum Corneum (SC) concentration distributions

The following compounds were present in more than 90% of the samples collected: octocrylene, homosalate, galaxolide, di-methyl phthalate, di-ethyl phthalate, di n-butyl phthalate, bis-2-ethyl hexyl phthalate, di-octyl terephthalate and squalene, as indicated in Table 1. For the compounds measured in more than 50% of the samples, we include the median and mean concentrations. Additional statistics for all wipes are included in the Supporting Information.

In comparing the magnitude of the standard deviations to the mean values listed in Table 1, we see a high variability in the concentrations across the subjects for many of the compounds. A high variability is apparent for most of the phthalates, including low molecular weight phthalates used in personal care products, and high molecular weight phthalates used as plasticizers and in building materials [45, 46]. This variability is likely explained by differences in concentrations to which people are exposed, as well as differences in use patterns of consumer products that contain these chemicals of interest. Squalene variability is quite significant among all subjects as well. The levels of squalene vary with age, because natural production by cells slows down starting at 30 years of age [47], skin conditions, such as acne [48], and also its possible presence as a moisturizer in some personal care products [49].

Analysis of squalene concentrations and estimation of depth of sampling.

Our samples presented higher levels of squalene, as summed between the three forehead wipes, than the upper bound values of skin levels reported in the literature from just one paper [41], which reported squalene measurements using a cup with the solvent hexane held up to the skin, and may have extracted squalene less effectively.

With all squalene concentrations from every subject and assuming a constant concentration with depth, we calculated the log-normal mean depth of wipe sample extraction (see SI). We estimate that the first wipe removed chemicals from the first 0.6 μm of the SC (SD: 0.3–1.1 range), the second wipe removed chemicals from 0.6 to 0.9 μm, an additional depth of 0.3 μm (SD: 0.2–0.5), and the third wipe removed chemicals from 0.9 to 1.1 μm, an additional 0.2 μm depth (SD: 0.1–0.4). The use of squalene to estimate the depth of sampling has limitations. There is both variability in squalene levels between subjects and also by body location [41]. As a result, the assumption of a constant squalene concentration to estimate the depth of sampling may produce depths that do not reflect the true sampling depth given that each subject has different levels. Moreover, a high inter-subject variability in the depth

of sampling due to the use of squalene as a marker may be expected; this variability may be compounded by the small sample size of the present study.

Analysis of the depth patterns of the chemicals

To further understand transport processes through skin, we investigated the concentration patterns of both SVOCs and squalene with each subsequent wipe. Because sequential wipes extract chemicals deeper in the SC, we determined the correlation between the estimated depth and concentration levels for every subject., Results are shown in Table 2. We also note the low values of the SD relative to the average correlation coefficients. The first column is the correlation coefficient of the concentration with depth for each SVOC, and the results are all negative, indicating that the compounds diffuse through the skin towards the dermis with a decreasing concentration pattern with depth.

The two compounds with the largest correlation coefficients out of the compounds assessed are di-methyl and di-ethyl phthalate indicating that they penetrate more deeply into the skin over shorter time periods and are found in higher concentrations at depth compared to the other SVOCs. There is a strong negative correlation for homosalate, octocrylene and galaxolide, indicating a steep decline with depth. The same holds true for bis-(2-ehtylhexyl) phthalate and di-octyl phthalate.

For squalene, there is a high variability in the observed levels among subjects, given its inherent biological variability The negative concentration gradient of squalene reflects that squalene is a major constituent of sebum but not keratinocytes, and by moving deeper into the SC the ratio of sebum-to-keratinocytes-related substances decreases [39], therefore the squalene concentrations should be decreasing. There is not a perfect correlation ρ between squalene and depth because of the calculation process. P represents the average correlation across all subjects between individual squalene levels and a common estimated depth, which is in turn the geometric mean across all subjects by using an assumed, constant squalene concentration. Sapienic acid (cis-6-hexadecenoic acid), which is a unique human lipid, makes up about 5.6% [41] of the total human skin lipids. It shows a strong negative gradient with depth across all 13 subjects (Table 2).

Table 2 also lists the average percent and the range of chemical load in the uppermost wipe, calculated by summing the total mass of chemicals removed from FH-1, FH-2 and FH-3 and dividing the recovered mass in FH-1 by the total mass. FH-1 removes between 40–65% of chemical, averaging 50%. For the compounds that exhibit a significant concentration gradient with depth, the percentage removed by FH-1 should be greater than for other compounds, since these compounds do not diffuse as much through the SC, with a low percentage of removal by subsequent forehead wipes. We note that there is a correlation between the percentage of chemical load in FH-1, the variation with depth, ρ, and the chemical properties of the compound, as represented by D_{SC}. For instance, the two compounds with the largest diffusion coefficients (D_{SC}), di-methyl and di-ethyl phthalates, have concentration gradients that are not statistically significant with depth, reflecting more even distribution throughout the SC, and as such, are removed to a greater extent by subsequent forehead wipes and making the chemical load in FH-1 lower.

However, the remaining obstacle is to distinguish whether each subsequent wipe extracted chemicals from deeper skin layers or they represented sequential extractions from the same depth stemming from differential solubility in isopropanol. We postulate that the amount of chemical extracted in skin from sequential wipes provides evidence of penetration depth and support this assumption with the following observations. First, the skin oils, squalene and sapienic acid, that are excreted by skin glands, are known to have decreasing concentration with depth, and both show a similar pattern of decreasing recovery with sequential hand wipes. The similarity in extraction between these compounds, despite their expected differences in solubility in isopropanol, are a strong argument that the wipes are physically removing skin cells rather than simply solubilizing compounds. Second, we also see variations in sequential chemical wipe extractions across different chemicals consistent with chemical properties, and similarities across subjects for a given chemical. These findings are more consistently explained by differences in skin diffusion (reflecting permeation) rather than by differences in solubility within isopropanol. For example, as shown in Table SI-5, the compounds dimethyl phthalate and diethyl phthalate are extracted in almost equal amounts in all three sequential wipes, even though these compounds are expected to be more soluble in organic solvents than is squalene (https://pubchem.ncbi.nlm.nih.gov). Squalene shows very different pattern with a large extraction in the first wipe. What is different about the phthalates is their greater diffusion coefficient in skin.

Model results.

The model has two components, transfer from the air to skin and diffusion through the skin. For 9 of the 14 compounds, the surface of the skin can reach 85% of the equilibrium concentration in less than one hour (Table SI-3), much less than the assumed 24-hour exposure period, and thus for these compounds the air to skin transfer rate does not control the resulting profile through the skin. Additionally, some compounds we measured may have been applied directly to skin, bypassing the partitioning step. Therefore, we use the model to calculate the concentration profile in the skin after 24 hours of exposure to a constant air concentration, calculated based on the measured skin's concentration in FH-1 and the K_{lg} of each compound. For one compound, DEHP, the time for the skin surface to reach equilibrium with air is 2.8 hours, and thus the assumption of constant air concentration on the skin surface can still be acceptable for modeling purposes. For homosalate, galaxolide, di-n-octyl phthalate and di-n-octyl terephthalate , the time for the skin surface to reach equilibrium with the air exceeds the 24-hour model simulation period, limiting the transfer through the dermal pathway. For these compounds, it is assumed that the skin surface is cleaned every 24 hours, and thus their concentration profiles in the skin driven by diffusion are not relevant. It has to be noted, however, that in other models [8], the primary factor driving transdermal permeability is the diffusion through the air boundary layer. In this model, no boundary layer was included, which may be responsible for the differences. Also, the equations employed to calculate K_{lg}, makes our values lower than those reported previously [8], which may explain why equilibrium air-to-skin was reached faster in our model, carrying through to the modeled concentration profiles. Further, the thickness of the outer layer of skin reaching equilibrium drives the time to equilibrium, and the thickness of this equilibrium surface is not well defined.

Figure 1 provides the resulting concentration profiles where the thicker line represents the model prediction and the other lines represent measured concentrations for each individual subject. We report the modeled normalized concentrations in the skin as a percentage of the concentration calculated in the uppermost wipe (FH-1) and compare the modeled estimates to the normalized measured concentrations in the wipes in Table 4. The compounds are listed in order of descending calculated diffusion coefficient, D_{SC} , and we see that the modeled concentrations are driven primarily by this property. The two compounds with the highest D_{SC}, present the highest surface-normalized concentrations at depth, which indicates that they migrate through skin faster than others due to their chemical properties and are at greater concentrations in subsequent wipes.

In combining the times to equilibrium obtained from the model and the wipes analysis, we observe that the compounds that reach equilibrium faster, also are found in higher percentages in subsequent wipes (2 and 3) (Table SI-5). From this fact, it can be hypothesized that, as equilibrium between air and skin lipids is faster, there is more time for the compound to diffuse through the skin, reaching deeper layers. Adding the diffusion coefficients to this discussion, as the D_{SC} increases, the permeability through the skin is greater, and chemicals. are extracted from deeper layers of the SC, as reflected in the measurements. Yet the different times to equilibrium for the chemicals also plays a role in the transport process through the skin and that explains why the order of chemicals by D_{SC} does not match perfectly the normalized modeled concentrations in Table 4. However, we also note that the two compounds with the highest D_{SC} values, are also two of the most likely to have been applied directly to skin, given their predominance in consumer products.

The model estimates regarding both partitioning and transport agree well with the interpretations gained from the chemical analyses measured in the wipes. Both results imply that the diffusion coefficient through the SC (D_{SC}) is a critical parameter needed to understand and predict the concentration profiles of different chemicals through the skin. However, because there are very few direct measurements of D_{SC}, we rely on estimation methods based on an empirical model statistically fit to available data provided in the US EPA Dermal Exposure Guidance to obtain this key parameter [35]. Increasing the number and reliability of D_{SC} measurements is needed to move forward on interpretation of both models and skin wipe measurements.

The results derived from the model are in terms of normalized concentrations, which make the impact and application of these results to other scenarios challenging. Also, it is worth pointing the overestimation of the model results due to the equilibrium calculations and assumptions. We also need to mention that, the fact of not considering skin surface lipids (SSL) as part of the skin, overestimates the model predictions since they act as an additional resistance to transport through skin [27]. Nonetheless, the qualitative model conclusions and the relationship of transport through the skin to chemical properties of the SVOCs is what can be considered when designing more refined and improved models.

Non-target approach for oxidation products identification.

With non-target methods, we tentatively identified three primary oxidation products formed by squalene ozonolysis [29]: 1-hydroxy-2-propanone (hydroxyacetone), 6-methyl-5-

hepten-2-one (6-MHO), and 6,10-dimethyl-5,9-undecadien-2-one (geranyl acetone). We subsequently confirmed these compounds using authentic standards. We found geranyl acetone in most wipes, but it did not exhibit a significant declining concentration pattern with depth as expected. We found 6-MHO in 1–3 wipes in most individuals, most often including the surface wipe. We only detected hydroxyacetone in one person. These compounds tend to be more volatile, and thus may escape into the gaseous phase [29], bypassing detection in the wipes.

From the LC-Q/TOF non-target analysis, we tentatively identified two oxidation products: 4,9,13,17-tetramethyl-octadeca-4,8,12,16-tetraenoic acid (C-22 tetraenoic acid) and 5,9,13-trimethyl-tetradeca-4,8,12-trienoic acid (C-17 trienoic acid). With no standards available, we did not make a full confirmation. However, the compounds were tentatively identified with fair confidence due to the following MS information: i) matching exact mass and isotope pattern of the precursor (confirmation of the molecular formula); ii) matching MS/MS fragments with predicted fragments from in-silico software tools (CFM-ID, MassFrontier). For C-17 trienoic acid, three MS/MS fragments were matched to the known spectrum, whereas for C-22 tetraenoic acid, only one MS/MS fragment was identified. More information regarding this analysis can be found in the SI.

We used the area under the curve as a proxy for the relative concentration in the wipes. From these data we could assess the decrease in concentration of the oxidation products in each wipe sample. We also calculated the linear correlation coefficient between the area under the curve and penetration depth of each wipe (Table 5). For C-22 tetraenoic acid, the concentration with each subsequent wipe was decreasing, implying that the ozonolytic reaction occurs closer to the skin surface and, as the next wipe extracts chemicals and skin lipids deeper from the skin, this relatively high K_{oa} compound partitions farther into skin. For C-17 trienoic acid, with a slightly lower K_{oa}, the trend did not reach statistical significance.

We tentatively identified two other oxidation products through the NIST Library in GC-Q/TOF (with no standards available for confirmation): C-17 trienal found on wipes from 4 people and C-22 tetraenal found on wipes from 5 people as summarized in Table 5.

Finally, we detected some other oxidation products similar in structure to compounds identified as potential oxidation products by Wisthaler and Weschler [29] in a small portion of the subjects, many times in a single participant. Based on their structures, these products are likely more volatile, so they tend to partition out of the skin and into the gas phase. We provide the compounds tentatively identified in the SI.

In conclusion, squalene measurements offer key insights for interpreting dermal wipe samples while measurements of its oxidation products provide valuable information about the production and fate of these respiratory and skin irritant products in the dermal layer. Further work is needed to identify these compounds reliably, subject to the constraint that there are not readily available standards, to better characterize their presence and relative levels, both in the skin and in the indoor environment. Further non-target analyses should be performed to identify related compounds in the wipes, as well as SVOCs and other

anthropogenic oxidation products, and propose pathways of oxidation other than ozone, such as microbes in the skin, or other processes that may alter and transform their original chemical structures.

Supplementary Material

Refer to Web version on PubMed Central for supplementary material.

Acknowledgments

Research reported in this publication was supported by the U.S. Environmental Protection Agency (EPA-G2013-STAR-K1), UC Davis Superfund Research Center, National Institutes of Health, NIEHS award (P42-ES004699) and the La Caixa Fellowship Program (“Obra Social La Caixa” from Spain).

REFERENCES:

1. Weschler CJ, Nazaroff WW Semi-volatile organic compounds in indoor environments. Atmospheric Environ. 2008, 42(40): 9018–9040.
2. van der Veen I, de Boer J Phosphorous flame retardants: properties, production, environmental occurrence, toxicity and analysis. Chemosphere. 2012, 88(10): 1119–1153. [PubMed: 22537891]
3. Kim YR, Harden FA, Toms LML, Norman RE Health consequences of exposure to brominated flame retardants: A systematic review. Chemosphere. 2014, 106: 1–19. [PubMed: 24529398]
4. Braun JM, Sathyanarayana S, Hauser R Phthalate exposure and children’s health. Curr Opin Pedr. 2013, 25(2): 247–254.
5. Benjamin S, Masai E, Kamimura N, Takahashi K, Anderson RC, Faisal PA Phthalates impact human health: Epidemiological evidences and plausible mechanism of action. J. Haz. Mater 2017, 340: 360–383.
6. Ruszkiewicz JA, Pinkas A, Ferrer B, Peres TV, Tsatsakis A, Aschner M Neurotoxic effect of active ingredients in sunscreen products, a contemporary review. Toxicology Reports, 2017, 4: 245–259. [PubMed: 28959646]
7. Xue J, Zartarian V, Moya J, Freeman N, Beamer P, Black K, Tulve N, Shalat S A meta-analysis of children's hand-to-mouth frequency data for estimation nondietary ingestion exposure. Risk Anal., 2007, 27(2):411–420. [PubMed: 17511707]
8. Weschler CJ, Nazaroff WW SVOC exposure indoors: fresh look at dermal pathways. Indoor Air. 2012, 22(5): 356–377. [PubMed: 22313149]
9. Beydon D, Payan JP, Grandclaude MC Comparison of percutaneous absorption and metabolism of di-n-butylphthalate in various species. Toxicology in vitro: an international journal published in association with BIBRA. 2010, 24(1):71–78. [PubMed: 19735722]
10. Weschler CJ, Nazaroff WW Dermal Uptake of Organic Vapors Commonly Found in Indoor Air. Environ. Sci. Technol 2014, 48 (2): 1230–1237. [PubMed: 24328315]
11. Weschler CJ, Bekö G, Koch HM, Salthammer T, Schripp T, Toftum J, Clausen G Transdermal uptake of diethyl phthalate and di(n-butyl) phthalate directly from air: experimental verification. Environ Health Perspect. 2015, 123(10):928–934. [PubMed: 25850107]
12. Prausnitz MR, Langer R Transdermal Drug Delivery. Nature Biotechnol. 2008, 26(11): 1261–1268. [PubMed: 18997767]
13. Rauma M, Boman A, Johanson G Predicting the absorption of chemical vapours. Adv Drug Deliv Rev. 2013, 65(2): 306–314. [PubMed: 22465561]
14. Rehal B, Maibach H Percutaneous absorption of vapors in human skin. Cutam Ocul Toxicol. 2011, 30(2):87–91.
15. Piotrowski J Further investigations on the evaluation of exposure to nitrobenzene. Brit. J. Ind. Med 1967, 24(1):60–65. [PubMed: 6017140]

16. Piotrowski J Evaluation of exposure to phenol: Absorption of phenol vapour in the lungs and through the skin and excretion of phenol in urine. Brit. J. Ind. Med 1971, 28(2):172–178. [PubMed: 5572685]
17. Jones K, Cocker J, Dodd LJ & Fraser I Factors affecting the dermal absorption of solvent vapours: A human volunteer study. Ann. Occup. Hyg 2003, 47(2), 145–150. [PubMed: 12581998]
18. Brooke L, Cocker J, Delic JL, Payne M, Jones K, Gregg NC, Dyne D Dermal uptake of solvents from the vapour phase: an experimental study in humans. Ann Occup Hyg. 1998, 42(8):531–40. [PubMed: 9838866]
19. Bader M, Wrbitzky R, Blaszkewicz M, Schaper M, van Thriel C Human volunteer study on the inhalational and dermal absorption of N-methyl-2-pyrrolidone (NMP) from the vapour phase. Arch. Toxicol. 2008, 82(1):13–20. [PubMed: 17721780]
20. Bekö G, Morrison GC, Weschler CJ, Koch HM, Pälmke C, Salthammer T, Schripp T, Eftekhari A, Toftum J, Clausen G G. Dermal uptake of nicotine from air and clothing: Experimental verification. Indoor Air. 2018, 28(2):247–257. [PubMed: 29095533]
21. Morrison GC, Bekö G, Weschler CJ, Schripp T, Salthammer T, Hill J, Anderson AA, Toftum J, Clausen G, Frederiksen H Dermal Uptake of Benzophenone-3 from Clothing. Environ Sci Technol. 2017, 51(19): 11371–11379. [PubMed: 28858503]
22. Morrison GC, Bekö G, Weschler CJ, Schripp T, Salthammer T, Hill J, Anderson AA, Toftum J, Clausen G, Frederiksen H Dermal Uptake of Benzophenone-3 from Clothing. Environ Sci Technol. 2017, 51(19): 11371–11379. [PubMed: 28858503]
23. Bekö G, Morrison GC, Weschler CJ, Koch HM, Palmke C, Salthammer T, Schripp T, Toftum J, Clausen G Measurements of dermal uptake of nicotine directly from air and clothing. Indoor Air. 2017, 27(2): 427–433. [PubMed: 27555532]
24. Gong MY, Zhang YP, Weschler CJ Predicting dermal absorption of gas-phase chemicals: transient model development, evaluation, and application. Indoor Air. 2014, 24(3): 292–306. [PubMed: 24245588]
25. Xu Y, Elaine A, Hubal C, Clausen PA, Little JC Predicting residential exposure to phthalate plasticizer emitted from vinyl flooring: a mechanistic analysis. Environ Sci Technol. 2009, 43(7): 2374–2380. [PubMed: 19452889]
26. Lorber M, Weschler CJ, Morrison G, Bekö G, Gong M, Koch HM, Salthammer T, Schripp T, Toftum J, Clausen G Linking a dermal permeation and an inhalation model to a simple pharmacokinetic model to study airborne exposure to di(n-butyl) phthalate. J Expo Sci Environ Epidemiol. 2016, 27(6): 601–609. [PubMed: 27531370]
27. Morrison GC, Weschler CJ, Bekö G Dermal uptake directly from air under transient conditions: advances in modeling and comparisons with experimental results for human subjects. Indoor Air. 2016, 26(6): 913–924. [PubMed: 26718287]
28. Weschler CJ Roles of the human occupant in indoor chemistry. Indoor Air. 2016, 26(1): 6–24. [PubMed: 25607256]
29. Wisthaler A, Weschler CJ Reactions of ozone with human skin lipids: Sources carbonyls, dicarbonyls and hydroxycarbonyls in indoor air. PNAS. 2010, 107(15): 6568–6575. [PubMed: 19706436]
30. Fooshee DR, Aiona PK, Laskin A, Laskin J, Nizkodorov SA, Baldi PF Atmospheric oxidation of squalene: Molecular study using COBRA Modeling and High Resolution Mass Spectrometry. Environ. Sci Technol. 2015, 49 (22): 13304–13313. [PubMed: 26492333]
31. Morrison GC Recent Advances in Indoor Chemistry. Curr Sustainable Renewable Energy Rep. 2015, 2:33–40.
32. Anderson SE, Franko J, Jackson LG, Wells JR, Ham JE, Meade BJ Irritancy and allergic responses induced by exposure to the indoor air chemical 4-oxopentanal. Toxicol Sci. 2012, 127(2): 371–38. [PubMed: 22403157]
33. Lakey PSJ, Wisthaler A, Berkemeier T, Mikoviny T, Poeschl U, Shiraiwa M Chemical kinetics of multiphase reactions between ozone and human skin lipids: Implications for indoor air quality and health effects. Indoor Air. 2016, 27(4): 1–13.
34. Gong MY, Zhang YP, Weschler CJ Measurement of phthalates in skin wipes: estimating exposure from dermal absorption, Environ. Sci. & Technol 2014, 48 (13), 7428–7435. [PubMed: 24911978]

35. U.S. EPA. (2007). Dermal Exposure Assessment: A Summary of EPA Approaches. U.S. Environmental Protection Agency, Washington, DC, EPA/600/R-07/040F.
36. Moschet C, Anumol T Lew BM, Bennett DH, Young TM Household Dust as a Repository of Chemical Accumulation: New Insights from a Comprehensive High-Resolution Mass Spectrometric Study. Environ. Sci. Technol 2018, 52 (5): 2878–2887. [PubMed: 29437387]
37. Moschet C, Anumol T, Hasenbein S, Lew BM, Young TM LC- and GC-QTOF/MS as Complimentary Tools for a Comprehensive Micropollutant Analysis in Aquatic Systems. Environ. Sci. Technol 2017, 51(3): 1553–1561. [PubMed: 28026950]
38. National Institute of Standards and Technology. NIST Standard Reference Database 1A, http://www.nist.gov/srd/nist1a.cfm (accessed September 27, 2017).
39. Nicolaides N Skin lipids: their biochemical uniqueness. Science. 1974, 186(4158): 19–26. [PubMed: 4607408]
40. Porro MN, Passi S, Boniforti L, Belsito F Effects of aging on fatty acids in skin surface lipids. J Invest Dermatol. 1979, 73(1): 112–117. [PubMed: 448170]
41. Greene RS, Downin DT, Pochi PE, Strauss JS Anatomical variation in the amount and composition of human skin surface lipid. J Invest Dermatol. 1970, 54(3): 240–247. [PubMed: 5436951]
42. Thiele JJ, Weber SU, Packer L Sebaceous gland secretion is a major physiologic route of vitamin E delivery to skin. J Invest Dermatol. 1999, 113(6):1006–1010. [PubMed: 10594744]
43. Guy RH, Potts RO Penetration of industrial chemicals across the skin: a predictive model. Am. J. Ind. Med. 1993, 23(5): 711–719. [PubMed: 8506849]
44. Mitragotri S Modeling skin permeability to hydrophilic and hydrophobic solutes based on four permeation pathways. J. Control. Release 2003, 86(1): 69–92. [PubMed: 12490374]
45. Bornehag CG, Lundgren B, Weschler CJ, Sigsgaard T, Hagerhed LE, Sundell J Phthalates in Indoor Dust and Their Association with Building Characteristics. Environ. Health Perspect 2005, 113(10): 1399–1404. [PubMed: 16203254]
46. Wensing M, Uhde E, Salthammer T. Plastic additives in the indoor environment—flame retardants and plasticizers. Sci. Total Environ. 2005, 339(1–3): 19–40. [PubMed: 15740755]
47. Pappas A. Lipids and skin health. Springer International Publishing AG Cham, Switzerland 2015.
48. Pappas A, Johnsen S, Liu JC, Eisinger M Sebum analysis of individuals with and without acne. Dermatoendocrinol. 2009, 1(3): 157–161. [PubMed: 20436883]
49. Sethi A,Kaur T, Malhotra SK, Gambhir ML Moisturizers: The Slippery Road. Indian J Dermatol. 2016, 61(3): 279–287. [PubMed: 27293248]

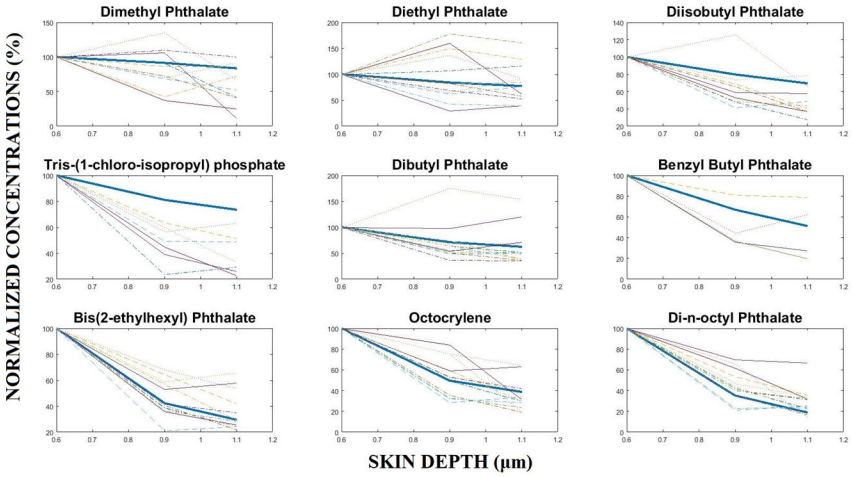

Figure 1.

Comparison of the results of the model (thicker line) to the measured concentrations in the wipes (thinner lines) through normalization of the concentrations, both measured and modeled, to the modeled and measured surface wipe FH-1 concentrations (%), with the calculated depth estimates (in µm).

Table 1.

Compounds detected in the wipes and their chemical properties. Percent of detection in the FH-1, mean, median and SD of the levels measured in the FH-1 along with CV are shown, .

Chemical properties				FH-1	Mean	Median	SD	CV[3]
Compound (Class)[1]	[2]Molecular weight (g/mol)	[2]Log K_{ow}	[2]H (mol/ Pa*m^3)	Detection %	µg/m^2	µg/m^2	µg/m^2	%
Di-methyl phthalate (PH)	194.18	1.56	0.020	100	9	8	5	56
Di-ethyl phthalate (PH)	222.30	2.47	0.045	100	1074	1046	526	49
Tris-1-chloro isopropyl phosphate (OP)	327.56	2.59	0.006	92	93	21	113	122
Tri-n-butyl phosphate (OP)	266.32	4.00	0.142	38	11	10	8	73
Di-isobutyl phthalate (PH)	278.34	4.11	0.124	92	454	344	347	76
Di-n-butyl phthalate (PH)	278.34	4.46	0.239	100	279	276	79	28
Galaxolide (MU)	258.41	5.90	13.172	92	169	52	240	140.0
Benzyl Butyl phthalate (PH)	312.36	4.84	0.132	62	113	112	39	34
Tri-phenyl phosphate (OP)	326.29	4.59	0.334	38	165	30	210	127
Homosalate (UV)	262.35	6.16	1.956	100	103924	369	141	0.1
Bis-(2-ethyl hexyl) phthalate (PH)	390.56	5.11	1.115	100	5911	4953	2956	50
Octocrylene (UV)	361.48	6.88	*3.04E-04	100	26099	230	371	1.4
Di-n-octyl terephthalate (PH)	390.56	8.54	1.195	100	11093	5044	9800	88
Di-n-octyl phthalate (PH)	390.56	8.10	0.263	74	74	-	104	140
Acetyl tributyl citrate (PL)	402.48	4.92	*3.83E-05	54	640	281	529	83
Bis-(2-ethyl hexyl) adipate (PL)	370.58	8.12	*8.98E-05	38	-	-	-	-
Squalene (SL)	410.73	*14.6	-	100	1704271	1540357	722652	42
Sapienic Acid (cis-6-hexadecenoic acid) (SL)	254.41	*6.74	-	100	3025144	1287368	5971791	197

1. Class to which the chemical belongs. UV: UV-protection compound; MU: musk; PL: plasticizer; PH: phthalate; OP: Organophosphorous flame retardant; SL: skin lipid.

2. These chemical properties have been obtained from NIST MS Library. When missing (*), log Kow and H have been estimated with EPI™.

3. CV: defined as coefficient of variation, equals: (SD/mean)*100

Table 2.

Correlation coefficients, ρ, of the chemical concentrations with depth of each forehead wipe and p-values associated through a Fisher's transformation. The percentage of chemical load (calculated by dividing the mass determined in FH-1 by the total mass of chemical measured in all three wipes) removed by FH-1 is shown as well.

Compound[1]	Mean ρ	SD ρ	p-value	% FH-1
Di-methyl phthalate	−0.33	0.76	0.342	39% (29-49)
Di-ethyl phthalate	−0.29	0.71	0.378	39% (28-50)
Tris-(1-chloro-isopropyl) phosphate	**−0.95**	**0.053**	**<0.001**	**47% (33-61)**
Di-isobutyl phthalate	**−0.90**	**0.16**	**<0.001**	**46% (31-61)**
Di-n-butyl phthalate	**−0.66**	**0.63**	**0.0013**	**47% (35-59)**
Galaxolide	**−0.96**	**0.048**	**<0.0001**	**49% (40-58)**
Benzyl Butyl phthalate	−0.93	0.10	0.114	53% (39-67)
Homosalate	**−0.93**	**0.098**	**<0.0001**	**56% (44-68)**
Bis-(2-ethylhexyl) phthalate	**−0.95**	**0.049**	**<0.001**	**59% (44-74)**
Octocrylene	**−0.95**	**0.040**	**<0.0001**	**51% (34-65)**
Di-n-octyl terephthalate	**−0.96**	**0.031**	**<0.001**	**65% (49-81)**
Acetyl tributyl citrate	**−0.96**	**0.029**	**0.0008**	**62% (55-69)**
Squalene	**−0.79**	**0.52**	**<0.001**	**52% (37-67)**
Sapienic Acid (cis-6-hexadecenoic acid)	**−0.91**	**0.16**	**<0.001**	**51% (38-64)**

[1]The compounds for which the chemical load and correlation coefficients were calculated are those with the highest percent of detection (> 50%) in the three forehead wipes. Bold text indicates statistically significant correlations ($p<0.05$).

Table 3.

Parameters used in the model.

COMPOUND[1]	[2] $\log K_{lg}$	[3] k_p (m/s)	[4] D_{sc} (m^2/s)
Di-methyl phthalate	2.9	4.4E-09	1.8E-15
Di-ethyl phthalate	3.9	1.3E-08	6.7E-16
Tris (1-chloro-isopropyl) phosphate	3.1	3.7E-09	1.4E-16
Tri-n-butyl-phosphate	5.5	8.7E-08	1.3E-16
Di-isobutyl phthalate	5.5	8.8E-08	1.0E-16
Di-n-butyl phthalate	6.1	1.5E-07	8.1E-17
Galaxolide	8.9	2.2E-06	4.1E-17
Benzyl Butyl Phthalate	6.1	1.8E-07	3.9E-17
Triphenyl phosphate	6.3	9.8E-08	3.8E-17
Homosalate	8.2	3.1E-06	3.2E-17
Bis (2-ethylhexyl) phthalate (DEHP)	7.2	9.3E-08	1.1E-17
Octocrylene	5.0	2.5E-06	5.0E-18
Di n-octyl terephthalate	8.8	1.2E-05	1.5E-18

1. The compounds modeled exclude some of the compounds detected in the wipes, such as Acetyl Tributyl citrate, Bis-(2-ethyl hexyl) adipate, and di-octyl terephthalate.

2. Klg= lipid-gas partition coefficient (no units). Calculated using an equation from the EPA Dermal Exposure Assessment [35]; equation 1 in the S.I.

3. Kp= permeability coefficient of the chemical through the stratum corneum (SC). Obtained from equations from the US EPA [35]; Equation 3 in the S.I.

4. Dsc= diffusion coefficient of the chemical through the stratum corneum (SC). Equation 4 in S.I.

Table 4.

Summary of model results; to the left, the first three columns represent modeled normalized concentrations to the first wipe closest to the surface (FH-1) after simulation in the model for 24 hours of exposure; to the right, the three columns represent the percentage of measured concentrations normalized to the FH-1 for each depth at which the wipe removes pollutant. Compounds modeled are ordered by descending D_{SC} value.

	Modeled normalized concentrations to modeled FH-1 (%) after 24 hours of exposure in the model			**Mean measured concentrations in the wipes normalized (%) to the measured concentration in FH-1 (SD)**		
Compound	**0.6 μm**	**0.9 μm**	**1.1 μm**	**0.6 μm**	**0.9 μm**	**1.1 μm**
Di-methyl phthalate	100	91.5	83.6	100	89.9 (29)	78.7 (42)
Di-ethyl phthalate	100	84.2	77.3	100	94.8 (47)	83.2 (37)
Tris (1-chloro-isopropyl) phosphate	100	81.1	73.5	100	78.2 (16)	69.9 (23)
Tri-n butyl phosphate	100	81.8	74.1	100	74.6 (17)	67.8 (20)
Di-isobutyl phthalate	100	79.8	69.5	100	71.1 (24)	65.8 (15)
Di-n-butyl phthalate	100	71.2	62.3	100	64.5 (35)	50.9 (38)
Galaxolide	100	55.4	43.2	100	49.0 (19)	35.8 (15)
Benzyl Butyl Phthalate	100	66.9	51.2	100	58.3 (25)	46.9 (28)
Triphenyl phosphate	100	66.3	49.8	100	56.4 (16)	37.3 (2)
Homosalate	100	65.2	47.8	100	61.9 (24)	37.8 (19)
Bis-(2-ethylhexyl) phthalate	100	42.3	29.5	100	46.9 (14)	37.1 (15)
Octocrylene	100	49.6	38.7	100	53.1(18)	36.9 (15)
Di-n-octyl terephthalate	100	35.2	18.9	100	44.6 (15)	30.7 (13)

Table 5.

Squalene oxidation products screened in the non-target analysis of the forehead wipes for both LC- and GC-Q/TOF, along with their estimated log K_{oa} through EPI Suite™ by using their SMILES fragments.

	Oxidation products	ID Score[1]	Meanρ	SD ρ	p-value	Number of subjects for whom the compound was detected in at least one wipe	Estimated log K_{oa}
LC-Q/TOF	C-17 trienoic acid ($C_{17}H_{28}O_2$)	87.27	−0.42	0.70	0.365	10	9.73
	C-22 tetraenoic acid ($C_{22}H_{44}O_2$)	96.19	−0.78	0.39	<0.001	9	11.39
GC-Q/TOF	1-hydroxy-2-propanone	Confirmed	-	-	-	1	2.72
	6-methyl -5-hepten-2-one	Confirmed	−0.96	0.03	0.345	10	4.27
	6,10-dimethyl-5,9-undecadien-2-one	Confirmed	−0.99	0.22	0.596	10	5.79
	C-17 trienal ($C_{17}H_{28}O$)	85.80	−0.94	0.39	0.679	4	7.38
	C-22 tetraenal ($C_{22}H_{44}O$)	81.20	−0.99	0.37	0.214	5	9.05

1. For LC-Q/TOF, the ID score refers to the Isotope Pattern Score. For GC-Q/TOF, it refers to NIST Library Match Factor.